

# Bisphosphonate Action

## Alendronate Localization in Rat Bone and Effects on Osteoclast Ultrastructure

Masahiko Sato, William Grasser, Naoto Endo, Robert Akins, Hollis Simmons, David D. Thompson, Ellis Golub, and Gideon A. Rodan

Department of Bone Biology and Osteoporosis Research, Merck Sharp & Dohme Research Laboratories, West Point, Pennsylvania 19486

### Abstract

Studies of the mode of action of the bisphosphonate alendronate showed that 1 d after the injection of 0.4 mg/kg [ $^3\text{H}$ ]alendronate to newborn rats, 72% of the osteoclastic surface, 2% of the bone forming, and 13% of all other surfaces were densely labeled. Silver grains were seen above the osteoclasts and no other cells. 6 d later the label was 600–1,000  $\mu\text{m}$  away from the epiphyseal plate and buried inside the bone, indicating normal growth and matrix deposition on top of alendronate-containing bone. Osteoclasts from adult animals, infused with parathyroid hormone-related peptide (1–34) and treated with 0.4 mg/kg alendronate subcutaneously for 2 d, all lacked ruffled border but not clear zone.

In vitro alendronate bound to bone particles with a  $K_d$  of  $\sim 1$  mM and a capacity of 100 nmol/mg at pH 7. At pH 3.5 binding was reduced by 50%. Alendronate inhibited bone resorption by isolated chicken or rat osteoclasts when the amount on the bone surface was around  $1.3 \times 10^{-3}$  fmol/ $\mu\text{m}^2$ , which would produce a concentration of 0.1–1 mM in the resorption space if 50% were released. At these concentrations membrane leakiness to calcium was observed. These findings suggest that alendronate binds to resorption surfaces, is locally released during acidification, the rise in concentration stops resorption and membrane ruffling, without destroying the osteoclasts. (*J. Clin. Invest.* 1991. 88:2095–2105.) Key words: bisphosphonates • osteoclasts • membrane permeability

### Introduction

Bisphosphonates are carbon-substituted pyrophosphate (PCP)<sup>1</sup> analogues that include potent inhibitors of bone resorption (1),

Dr. Simmons's and Dr. Thompson's present address is Pfizer Inc., Central Research Division, Box 272, Eastern Point Road, Groton, CT 06340. Dr. Akins's present address is Department of Biology, University of Pennsylvania, Philadelphia, PA 19104. Dr. Golub's present address is Department of Biochemistry, University of Pennsylvania, School of Dental Medicine, 4001 Spruce Street, A1, Philadelphia, PA 19174.

Address correspondence to Gideon A. Rodan, M. D., Ph. D., Department of Bone Biology and Osteoporosis Research, Merck Sharp & Dohme Research Laboratories, West Point, PA 19486.

Received for publication 3 March 1991 and in revised form 9 July 1991.

1. *Abbreviations used in this paper:* ABP, alendronate; APD, aminohydroxypropylidene bisphosphonate; EHDP, etidronate; PCP, carbon-substituted pyrophosphate; PTHrP, human parathyroid hormone-related peptide.

*J. Clin. Invest.*

© The American Society for Clinical Investigation, Inc.

0021-9738/91/12/2095/11 \$2.00

Volume 88, December 1991, 2095–2105

which have been effectively used to control osteolysis or reduce bone loss in Paget's disease (2–12), metastatic bone disease (13–17), hypercalcemia of malignancy (18–24), and osteoporosis (25–30). However, despite the widening acceptance of bisphosphonates as therapeutic agents, their mechanism of action remains largely unknown. Like pyrophosphate, bisphosphonates bind to hydroxyapatite and as a result are taken up by bone. Bisphosphonate inhibition of bone resorption was initially attributed to reduced hydroxyapatite dissolution (31); however, structure-activity relation studies showed no close correlation between the two actions and directed attention to their effects on bone cells (1). Proposed mechanisms of action include cytotoxic or metabolic injury of mature osteoclasts (32, 33), inhibition of osteoclast attachment to bone (34), inhibition of osteoclast differentiation or recruitment (35–39), or interference with osteoclast structural features (cytoskeleton) necessary for bone resorption (40–42). It was suggested that, although all bisphosphonates act selectively on bone because of their concentration in this tissue, their mechanism of action may differ according to their chemical structure (1).

The 4-amino-1-hydroxybutylidene-1,1-biphosphonic acid (alendronate) is a potent inhibitor of bone resorption in vitro (42) in experimental animals (43, 44) and in patients with Paget's disease (9, 11, 45, 46). To better understand its mode of action we examined in this study the association of [ $^3\text{H}$ ]alendronate with bone particles, its localization in rat bone (1 and 6 d after injection), its effect on osteoclast ultrastructure in situ, on rat and chicken osteoclast resorption in vitro, and on osteoclast intracellular calcium and cyclic AMP levels. The findings support the hypothesis that alendronate binds to sites of bone resorption, is locally released by acidification, which increases its local concentration under the osteoclasts and interferes with bone resorption and ruffled border formation.

### Methods

All reagents were obtained from Sigma Chemical Corp., St. Louis, MO, unless otherwise stated. Fura-2, Fura-2AM, BR-A23187 were from Molecular Probes, Inc., Eugene, OR. Dimethylsulfoxide under  $\text{N}_2$  was from Aldrich Chemical Co., Milwaukee, WI. Organic solvents were from Fisher Scientific Co., Malvern, PA, and fixatives from Electron Microscopy Sciences, Fort Washington, PA.

**[ $^3\text{H}$ ]Alendronate binding to human bone particles.** [ $^3\text{H}$ ]alendronate (25,000 cpm, 4.85  $\mu\text{Ci}/\mu\text{mol}$ ) was incubated with human bone powder (1 mg, 180 mesh) in a buffer containing 0.2 M Tris-formate, pH 7.0. The incubations were carried out in a 96-well filter manifold (Millipore Corp., Bedford, MA) at room temperature, and the reaction was terminated by application of vacuum. The filtrate was collected in a 96-well cluster dish, and aliquots were counted in a liquid scintillation counter (LKB Instruments, Inc., Gaithersburg, MD). The concentration of alendronate was adjusted by addition of unlabelled drug before the addition of the bone particles to the incubation mixture.

**[ $^3\text{H}$ ]Alendronate localization in rat bone.** Sprague-Dawley rats (1–2 d postpartum, weighing 4 g) were injected subcutaneously with 1.4–2

$\mu\text{g}$  of [butyl-2,3- $^3\text{H}$ ]alendronate at a specific activity of  $4 \mu\text{Ci}/\mu\text{mol}$ . Experimental animals and litter mate controls were killed at 1 and 6 d postinjection. Femora were dissected clean of soft tissue, split at the diaphysis, and flushed with 60 mM Pipes (Calbiochem-Behring Corp., San Diego, CA), 25 mM Hepes (pH 7.0), 2 mM EGTA, 2 mM  $\text{MgSO}_4$ , 2.5% glutaraldehyde for 1 h at  $4^\circ\text{C}$ , and postfixed in 2% osmium tetroxide for 1 h at room temperature. Alternatively, femurs were fixed in 60 mM sodium phosphate buffer (pH 7.0), 2 mM  $\text{MgSO}_4$ , 5 mM EGTA, 2% formaldehyde, 2.5% glutaraldehyde for 3 h at room temperature and postfixed in 1% osmium tetroxide, 1.5% potassium ferrocyanide (47) for 2 h at room temperature. The latter femurs were stained en bloc with 1% uranyl acetate for 2 h at room temperature, dehydrated through graded acetone solutions, and embedded in Spurr's resin.

Serial 0.4–0.5- $\mu\text{m}$  sections were cut on an Ultracut E microtome (Reichert-Jung, Vienna, Austria), transferred to glass slides (Fisher), which were dipped in Kodak NTB2 emulsion, diluted 1:1 with 0.6 M ammonium acetate, vertically dried for 2 h at room temperature, and then stored with desiccant at  $4\text{--}5^\circ\text{C}$  for 30–130 d. Sections were developed in Kodak D19 (1:1  $\text{H}_2\text{O}$ ). Sections were then stained with 0.5% toluidine blue, 1% sodium borate (pH 9.5) for 4 min at  $60^\circ\text{C}$ .

[ $^3\text{H}$ ]Alendronate localization was examined on sections from the distal metaphyses of right femurs. Surfaces were quantitated in 10 fields of the metaphysis, 150  $\mu\text{m}$  from the epiphyseal plate and the endocortical bone surface, using OsteoMeasure (Osteometrics, Inc., Atlanta, GA) interfaced with a Nikon Optiphot. Labeled surfaces were recognized by imaging silver grains in bright-field and reflected light microscopy (see Fig. 4). "Osteoclast surfaces" were defined as regions of bone beneath vacuolated, multinucleated cells flattened against trabecular bone. "Forming surfaces" were defined as regions with osteoid beneath a layer of cuboidal mononuclear cells. All other surfaces, including eroded and resting surfaces were pooled for the purpose of this analysis.

For electron microscopic autoradiography, serial 100-nm sections were placed onto slides precoated with 0.7% Formvar (Ted Pella, Inc., Reading, PA) in ethylene dichloride, carbon coated, and then processed as above. After development, sections were floated off in  $\text{H}_2\text{O}$  (or eight drops HF/40 ml  $\text{H}_2\text{O}$ ) (48), picked up with 150 mesh grids, cleared by floating the emulsion side on concentrated acetic acid for < 15 s, stained with 2.5% uranyl acetate for 10 min at room temperature and then lead citrate (49) for 2 min at room temperature. Grids were viewed at 80 kV on a Phillips CM12 microscope and photographed with Kodak 4482 film.

The long bones and plastic sections from neonatal rats injected with [ $^3\text{H}$ ]alendronate were flame oxidized in an oxygen combustor (306; Packard Instrument Co., Inc., Canberra Industries, Meriden, CT) and counted for [ $^3\text{H}$ ] in a scintillation counter (LKB).

*Estimation of amount of alendronate on the bone surface.* Bone slices of  $4.4 \text{ mm} \times 4.4 \text{ mm} \times 0.2 \text{ mm}$  or  $42.24 \text{ mm}^2$  total surface incubated with 1 ml 0.1  $\mu\text{M}$  alendronate at pH 7.2 adsorbed 50% of the alendronate from solution (estimated by radiotracer uptake). Assuming random distribution on the surface of the bone slice the density of alendronate should be  $1.25 \times 10^{-18} \text{ mol}/\mu\text{m}^2$ . An average size resorption pit (estimated from electron micrographs of bone in situ) of  $500 \mu\text{m}^2$  should contain 0.62 fmol. If 50% are released within an enclosed space beneath an osteoclast of  $500 \mu\text{m}^3$  the local concentration would be  $\sim 0.5 \text{ mM}$ .

We also tried to estimate the amount of alendronate under osteoclast surfaces in the sections examined by autoradiography. Incubation solutions monitored throughout sample processing contained no detectable radioactivity. The [ $^3\text{H}$ ]alendronate content was estimated in histological sections by combustion and [ $^3\text{H}$ ] counting. Considering the specific activity of 5 Ci/mmol, a counting efficiency of 50% and 100 cpm above background in 10 sections, each section contained  $\sim 2$  fmol alendronate. In the third of the section which was examined histomorphometrically, 22% of the label or 0.145 fmol was localized to  $233 \mu\text{m}^2$  of osteoclast surface, assuming that the "dense" labeling contains fivefold more alendronate than the "moderate" labeling (Fig. 4). Since the sections are 0.4  $\mu\text{m}$  thick alendronate density on the surface would be  $1.6 \times 10^{-18} \text{ mol}/\mu\text{m}^2$ . If 50% of the alendronate on the osteoclast surface

was released in a space 1  $\mu\text{m}$  deep, the local concentration would be  $\sim 0.8 \text{ mM}$ , which is in remarkable agreement with the estimate obtained from in vitro data for the pharmacologically effective concentration of 0.1  $\mu\text{M}$ .

*Osteoclast ultrastructure.* Adult Sprague-Dawley rats weighing 250 g were injected subcutaneously with 0.4 mg alendronate/kg 96 h before being killed. Starting at 48 h before killing, animals were infused with 60 pmol/h of human parathyroid hormone-related peptide [PTHrP(1-34) $\text{NH}_2$ ], using an implanted pump (1003D; Alza Corp., Palo Alto, CA). Rats were killed by perfusion via a catheter implanted into the abdominal aorta, with 0.1–0.2 ml heparin (1,000 U/ml; LymphoMed, Rosemont, IL), followed by 10 ml 0.1% sodium nitrite in PBS (pH 7.2), and then 40 ml of 2.5% glutaraldehyde, 0.1% sucrose, 0.1 M sodium cacodylate (pH 7.0) at  $5^\circ\text{C}$ . Tibiae were removed, cleaned of soft tissue, and decalcified for 2 wk at  $4^\circ\text{C}$  in 5 mM 3-[*N*-Morpholino]propane sulfonic acid (Mops) (pH 7.2), 0.1% glutaraldehyde, 4% EDTA followed by a 3-d rinse in 0.1 M Mops (pH 7.0) at room temperature. Samples were postfixed in 2% osmium tetroxide, 0.1 M Mops (pH 7.0), dehydrated through graded acetone solution, and then embedded in Spurr's resin. Sections of 130 nm were cut and examined with a Phillips CM12 microscope and photographed with Kodak 4482 film as described above.

*Osteoclast bone resorption in culture.* Osteoclasts were isolated from chickens by methods described by Zamboni-Zallone et al. (50) and Blair et al. (51). Medullary bone was harvested from split femora and tibiae of Dekalb XL laying hens maintained on a calcium deficient diet (5070C-9; Ralston-Purina Co., St. Louis, MO) for 2–4 wk. The bone suspension was washed in PBS at  $4^\circ\text{C}$ , pressed through a 110- $\mu\text{m}$  nylon mesh, incubated in 0.2% NaCl for 2 min at  $37^\circ\text{C}$  to lyse red blood cells, and then sedimented through a 70% serum gradient for 90 min at  $4^\circ\text{C}$ . The bottom 5 ml was resuspended over a three-step Nycodenz gradient (1.073, 1.099, 1.143  $\text{g}/\text{cm}^3$ ) (Accurate Chemical & Scientific Corp., Westbury, NY) and centrifuged (350 g) for 20 min at  $4^\circ\text{C}$ . Cells from below the first band to above the pellet were pooled and resuspended into  $\alpha$ -MEM (pH 7.00–7.2), 10% FCS, antibiotics (Gibco Laboratories, Grand Island, NY) plus 2–5  $\mu\text{g}/\text{ml}$  cytosine-1- $\beta$ -D-arabinofuranoside at  $4^\circ\text{C}$ . The cell suspension was aliquoted into plates (Costar Corp., Cambridge, MA) to yield 1,000–4,000 osteoclasts/ $\text{cm}^2$ .

Bone resorption was assayed as the  $^3\text{H}$ -cpm released from bone particles aliquoted at  $100 \mu\text{g}/\text{cm}^2$  onto chicken osteoclasts in 48-well plates (Costar Corp.). Bone particles (20–53  $\mu\text{m}$ ) were made by sieving crushed bone from rats injected with [ $^3\text{H}$ ]proline (Amersham Corp., Arlington Heights, IL) as described by Blair et al. (51).  $^3\text{H}$ -cpm released into the media was quantitated with a liquid scintillation counter (LKB Instruments, Inc.). Resorption was typically assayed between days 4–6 in culture.

Resorption by rat osteoclasts in culture was carried out as described in detail in Sato and Grasser (42) and Arnett and Dempster (52). Briefly, cells isolated from the long bones of 1–3-d old rats (Sprague-Dawley) were aliquoted onto  $4.4 \times 4.4 \times 0.2\text{-mm}$  bone slices from the diaphysis of bovine femur. After overnight incubation, resorption was assayed by removing cells, fixing bone slices, staining with toluidine blue, and quantitating resorption pits by reflected polarized light microscopy.

*Measurements of intracellular calcium.* Chicken and rat osteoclasts cultured on no. 1.5 cover slips (Fisher) were incubated for 40 min at  $16^\circ\text{C}$  in 10  $\mu\text{M}$  Fura-2AM in Jok2 (111.2 mM NaCl, 5.4 mM KCl, 1.5 mM  $\text{CaCl}_2$ , 1 mM  $\text{MgCl}_2$ , 2 mM  $\text{Na}_2\text{HPO}_4$ , 11.1 mM dextrose, 10 mM Hepes [pH 7.5], plus MEM amino acids and vitamins [Gibco]). Cells were rinsed and incubated in complete media ( $\alpha$ -MEM for chicken, 199 for rat) for 10 min,  $37^\circ\text{C}$ . Cover slips were inverted diagonally over a drop of Jok2 on a quartz coverslip ( $1 \times 1 \text{ in.}$ , Thomas Scientific, Swedesboro, NJ). The chamber was mounted onto a thermal stage (Sensortek, Clifton, NJ) with the quartz side down on a Nikon Diaphot and perfusion of preheated solutions ( $37^\circ\text{C}$ ) was initiated with strips of Whatman no. 1 filter paper (Fisher Scientific Co., Pittsburgh, PA). The peripheral cytoplasm of FURA-2 loaded osteoclasts, devoid of nuclei, was excited at 348/380 nm using a Deltascan system (PTI

[Photon Technology International Inc.], S. Brunswick, NJ). The fluorescence emission through a 490-nm long pass filter was measured with a photomultiplier interfaced with a computer with d1048 software (PTI). Osteoclasts were perfused with 0.1 mM alendronate in Jok2. Background spectra and calibration were carried out for each cell. Both rat and chicken osteoclasts were used within one day of isolation.

**Adenylate cyclase assays.** Chicken osteoclasts were incubated with 1  $\mu\text{Ci}$  [ $^3\text{H}$ ]adenine (New England Nuclear, Boston, MA) for 2 h at 37°C. Cells were then washed and incubated with 1 mM isobutyl methylxanthine in the absence or presence of 10  $\mu\text{M}$  to 0.1 mM alendronate for 10 min. [ $^3\text{H}$ ]cAMP was chromatographically separated from other nucleotides and counted as described by Salomon et al. (53).

## Results

**Alendronate binding to bone particles.** Incubation of [ $^3\text{H}$ ]alendronate with human bone particles in vitro resulted in rapid, reversible, saturable binding (Fig. 1). At pH 7 the apparent dissociation constant was  $\sim 1.0$  mM, and the binding capacity was estimated at 105 nmol alendronate bound/mg bone. Unlabelled alendronate and etidronate (EHDP) were equally effective in competing with the binding of [ $^3\text{H}$ ]alendronate to bone powder, suggesting that both bisphosphonates bind to the same sites with similar affinity (Fig. 2). When bone powder was incubated with 10  $\mu\text{M}$  alendronate at pH 7 and then was exposed to decreasing pH, increasing amounts of the previously bound alendronate were released, up to 50% at pH 3.5 (Fig. 3). Taken together, these data indicate that substantial amounts of alendronate accumulate on bone surfaces at physiological pH and that significant amounts could be released by acidification.

**[ $^3\text{H}$ ]Alendronate localization in rat bone.** Neonatal rats injected with [butyl-2,3- $^3\text{H}$ ]alendronate ([ $^3\text{H}$ ]alendronate) were killed after 1 and 6 d to ascertain retention and localization of [ $^3\text{H}$ ]alendronate in developing bones. Oxygen combustion of bone samples and scintillation counting showed that after 1 d the rats retained  $49.7 \pm 12.2\%$  of the injected [ $^3\text{H}$ ]alendronate.

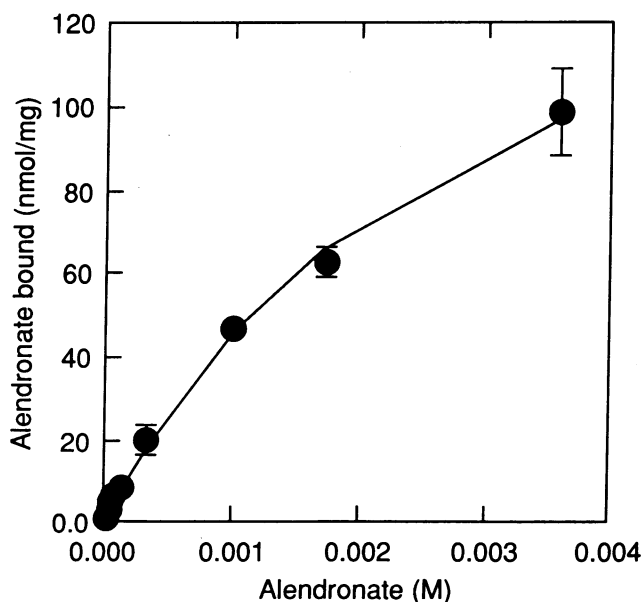


**Figure 1.** [ $^3\text{H}$ ]Alendronate binding to bone. An ultrafiltration assay was used to examine the binding of [ $^3\text{H}$ ]alendronate to human bone particles (180 mesh), as described in Methods. Each point is the mean  $\pm$  SD ( $n = 3$ ). These data suggest a dissociation constant of  $K_d = 1$  mM with a binding capacity of 105 nmol alendronate/mg bone.

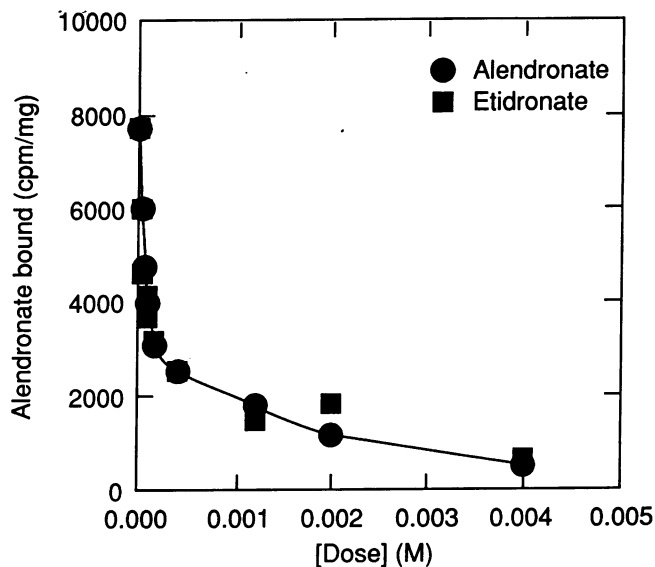


**Figure 2.** Inhibition of [ $^3\text{H}$ ]alendronate binding to bone by unlabelled alendronate or EHDP. [ $^3\text{H}$ ]Alendronate (8  $\mu\text{M}$ ) was equilibrated with unlabelled alendronate or EHDP and then binding to human bone particles (180 mesh) was determined as described in Methods (mean  $\pm$  SD) ( $n = 3$ ). The identical effects of excess alendronate and EHDP demonstrate that these bisphosphonates bind to human bone with similar affinities to the same sites.

Femora contained 0.045–0.12  $\mu\text{Ci}$  or 2.2–6 ng [ $^3\text{H}$ ]alendronate/femur. Sections of distal femoral metaphyses of 0.4–0.5  $\mu\text{m}$  contained 10 pCi or  $0.6 \pm 0.15$  pg [ $^3\text{H}$ ]alendronate/section.

Under light microscopy autoradiography these nondecalcified distal femur sections (Fig. 4) showed nonuniform labelling of mineralized surfaces, which ranged from dense labelling to near background. On many surfaces there was clearly above background labelling, which was divided into two levels for histomorphometric analysis: densely labelled surfaces where silver grains coalesced and were several layers deep, and moderately labelled surfaces where silver grains were separate from

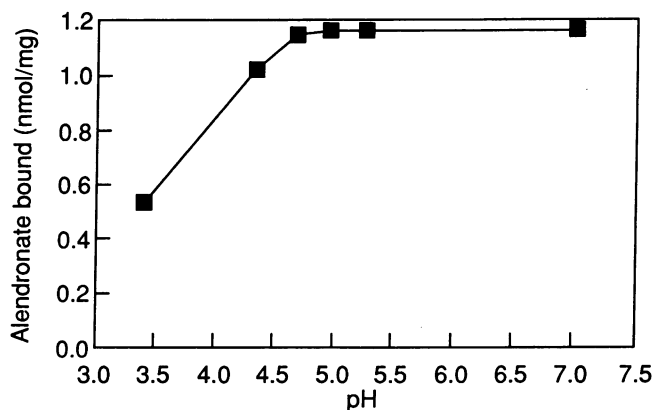


**Figure 3.** pH dependence of alendronate binding to human bone powder. [ $^3\text{H}$ ]Alendronate (10  $\mu\text{M}$ ) was incubated with human bone powder (180 mesh) in 0.1 M Tris-formate buffer maintained at differing pH. Acidification alone caused dissociation of the alendronate/bone complex,  $\sim 50\%$  of the alendronate being released at pH 3.5 (mean  $\pm$  SD) ( $n = 3$ ).



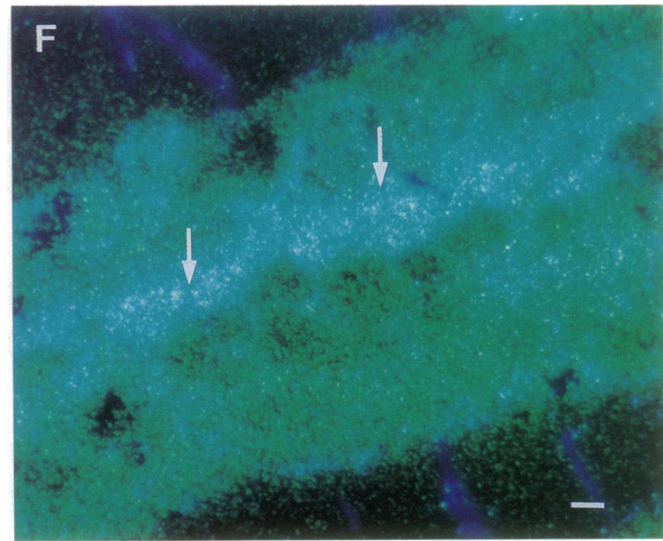
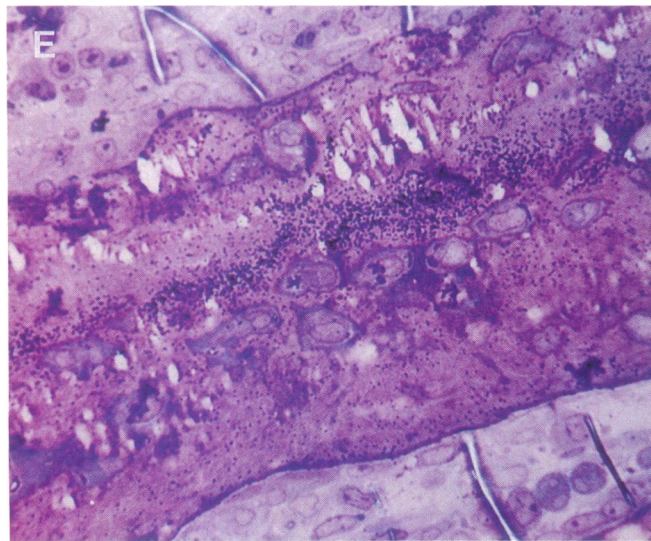
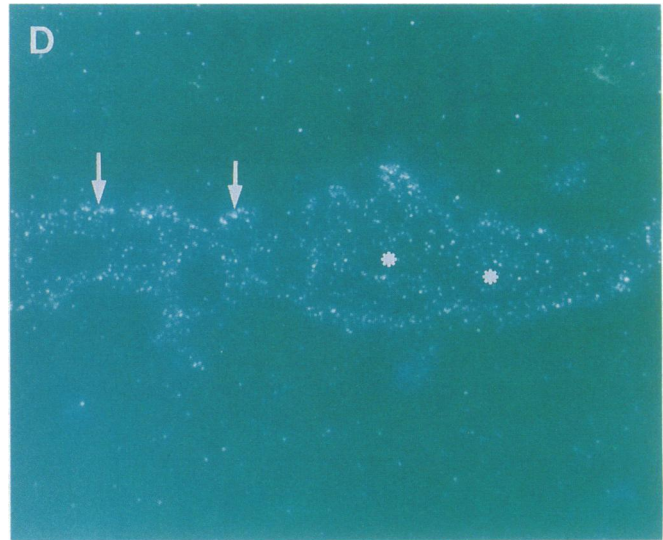
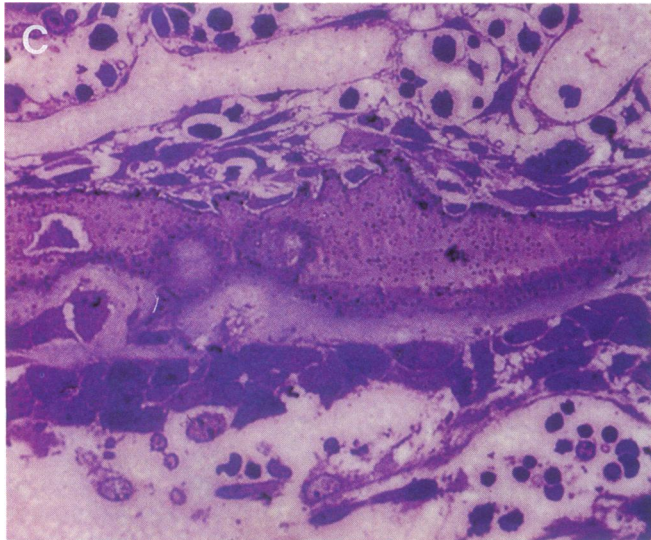
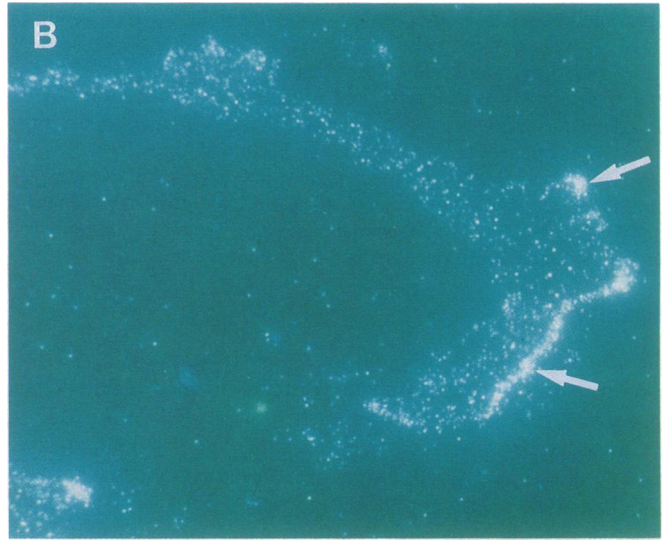
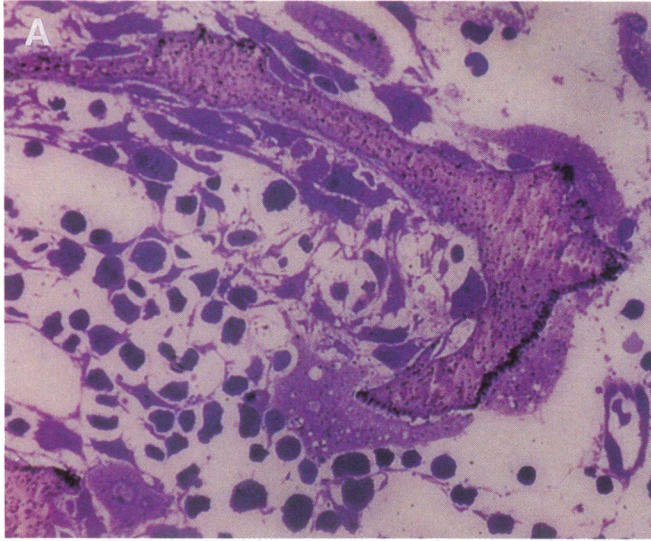


Table I. Histomorphometry of Sections (0.4  $\mu\text{m}$ ) from Rats 1 d after Injection with [ $^3\text{H}$ ] Alendronate

	Percent of total surface	Percent dense label	Percent moderate label	Percent sparse or unlabeled (by difference)
Osteoclast surface	4.5 $\pm$ 0.8	71.6 $\pm$ 0.8	0	28.4
Forming surface	47.8 $\pm$ 0.6	2.0 $\pm$ 5.0	46.4 $\pm$ 0.6	51.6
All other surfaces resting, eroded, etc.	47.7 (by difference)	12.8 $\pm$ 0.5	10.8 $\pm$ 0.5	76.4
Percent of total surface	100	10.28	27.3	62.4

Active resorbing surfaces were defined as scalloped regions of bone adjacent to active osteoclasts. Forming surfaces were regions adjacent to cuboidal osteoblasts. The remaining difference constituted resting surfaces. Also listed are the proportion of the labelling that was considered dense, moderate, and sparse, as described in the text.

each other. Dense labelling was seen primarily under osteoclasts (see arrow in Fig. 4) while moderate labelling was seen to a variable extent on all other surfaces (two arrows in Fig. 4), as described below. Histomorphometric analysis (Table I) of 15 sections of the distal femoral metaphyses (10 fields, 150  $\times$  150  $\mu\text{m}$  = 225,000  $\mu\text{m}^2$ , each) carried out by two independent investigators, showed that these sections contained  $\sim$  5% osteoclast surface, defined as identifiable osteoclasts in close apposition to bone;  $\sim$  48% active bone formation surfaces, defined as surfaces lined by osteoid and cuboidal osteoblasts. The other surfaces were not easily separable in the developing bone and were considered together for the analysis of the distribution of label. 24 h after [ $^3\text{H}$ ]alendronate injection 10.3% of the total bone surface was densely labelled and 27.3% moderately labelled. In this rapidly turning over bone most of the osteoclast surface, 71.6 $\pm$ 0.8% was densely labelled and 28.4% was unlabelled. On the other hand only 2% of the forming surfaces were densely labelled and 46.4% were moderately labelled. Of the other surfaces which contain resting and eroded surfaces, 12.8% were densely labelled and 10.8% moderately.

6 d after injection of 1.4  $\mu\text{g}$  [ $^3\text{H}$ ]alendronate into neonatal rats the animals still showed 45% retention of the injected dose and 4.9 ng [ $^3\text{H}$ ]alendronate per femur, not significantly different from 24-h postinjection levels. The labelled areas in these samples were 600–1,000  $\mu\text{m}$  away from the epiphyseal plate. Autoradiography of these femora showed a distinct layer of moderate [ $^3\text{H}$ ]alendronate labelling in the cortical bone and in discrete regions of trabecular bone that were no longer confined to the surface, thus no forming surfaces were labelled at this point (Fig. 4 C). These findings indicate bone formation on top of alendronate-labelled surfaces. The width of dense label estimated 1 d after [ $^3\text{H}$ ]alendronate injection was 20 $\pm$ 2.1  $\mu\text{m}$  and 6 d after tracer administration 23.5 $\pm$ 3.5  $\mu\text{m}$ , suggesting lack of diffusion through bone.

Autoradiography at the electron microscopic level showed absence of silver grains over all cells except osteoclasts. Osteoclasts were identified by the presence of multiple nuclei, abundant cytoplasm with numerous mitochondria, lysosomes, vacuoles, and ruffled borders. Over half the osteoclasts examined showed evidence of active bone resorption (57 $\pm$ 3%) and of those  $\sim$  80% were resorbing bone labelled with [ $^3\text{H}$ ]alendronate, consistent with the light microscopy observations. In many cases the ruffled borders were not sharply defined. Fig. 5 C shows silver grains along bone surfaces, beneath ruffled border and in vacuoles where 60% of the cellular labelling was observed. 40% of silver grains above osteoclasts were seen over the cytoplasm, nuclei and mitochondria. This [ $^3\text{H}$ ]alendronate is probably associated with the osteoclast cytoplasm, since the diffusible substances would have been lost through graded acetone treatment during tissue processing. These findings strongly suggest that during resorption osteoclasts cause the release and uptake of [ $^3\text{H}$ ]alendronate from the bone surface.

*Effect of alendronate on osteoclast ultrastructure.* In these experiments adult rats previously injected twice with the therapeutically effective dose of 0.4 mg/kg alendronate were infused for 2 d with the 1-34 fragment of PTHrP to stimulate bone resorption. Electronmicrographs of bone from control animals showed that all osteoclasts adjacent to bone (20 out of 20 encountered) had extensive ruffled borders and clear zones rich in actin filaments, indicative of active bone resorption. These cells were polymorphic, suggesting active motility, and had numerous vesicles associated with the ruffled border and vacuoles dispersed throughout the cytoplasm (Fig. 6). On the other hand, all osteoclasts adjacent to bone (20 out of 20) from alendronate-treated rats had considerably fewer vacuoles and lacked ruffled borders, although their membrane followed the contour of the bone surface. However, clear zones were apparent in several of these cells (Fig. 6). These findings suggest that

Figure 4. Autoradiography of rat femora 1 and 6 d postinjection. The distal metaphyses of femurs from rats injected with [ $^3\text{H}$ ]alendronate were processed for autoradiography after 1 (A–D) and 6 (E, F) days postinjection. Bright-field (A, C, E) and corresponding reflected light micrographs (B, D, F) were recorded for 10 fields 150  $\mu\text{m}$  from the epiphyseal plate and 150  $\mu\text{m}$  from the endocortical surface. Three levels of trabecular bone labelling were observed including dense (heavy arrows, B), moderate (light arrows, D–F) and sparse labelling (\*, D), the latter was near background in intensity. A majority (57%) of the total osteoclasts observed (heavy arrows in A and B) appeared to be active in resorption and most (83%) of the resorbing surfaces were labelled with [ $^3\text{H}$ ]alendronate. Reflected light microscopy showed intracellular labelling of active osteoclasts (A, B) but not of other cells. 6 d postinjection sections showed labelling  $\sim$  1 mm below the epiphyseal plate. Labelling was still observed over 11% of the total bone surface but much of the label was embedded in trabecular bone (E, F). The width of the labelling and total [ $^3\text{H}$ ] counts/section or femur were not significantly different from 1-d animals, suggesting limited diffusion and a long half-life for [ $^3\text{H}$ ]alendronate in vivo. Micrometer: 10  $\mu\text{m}$ .



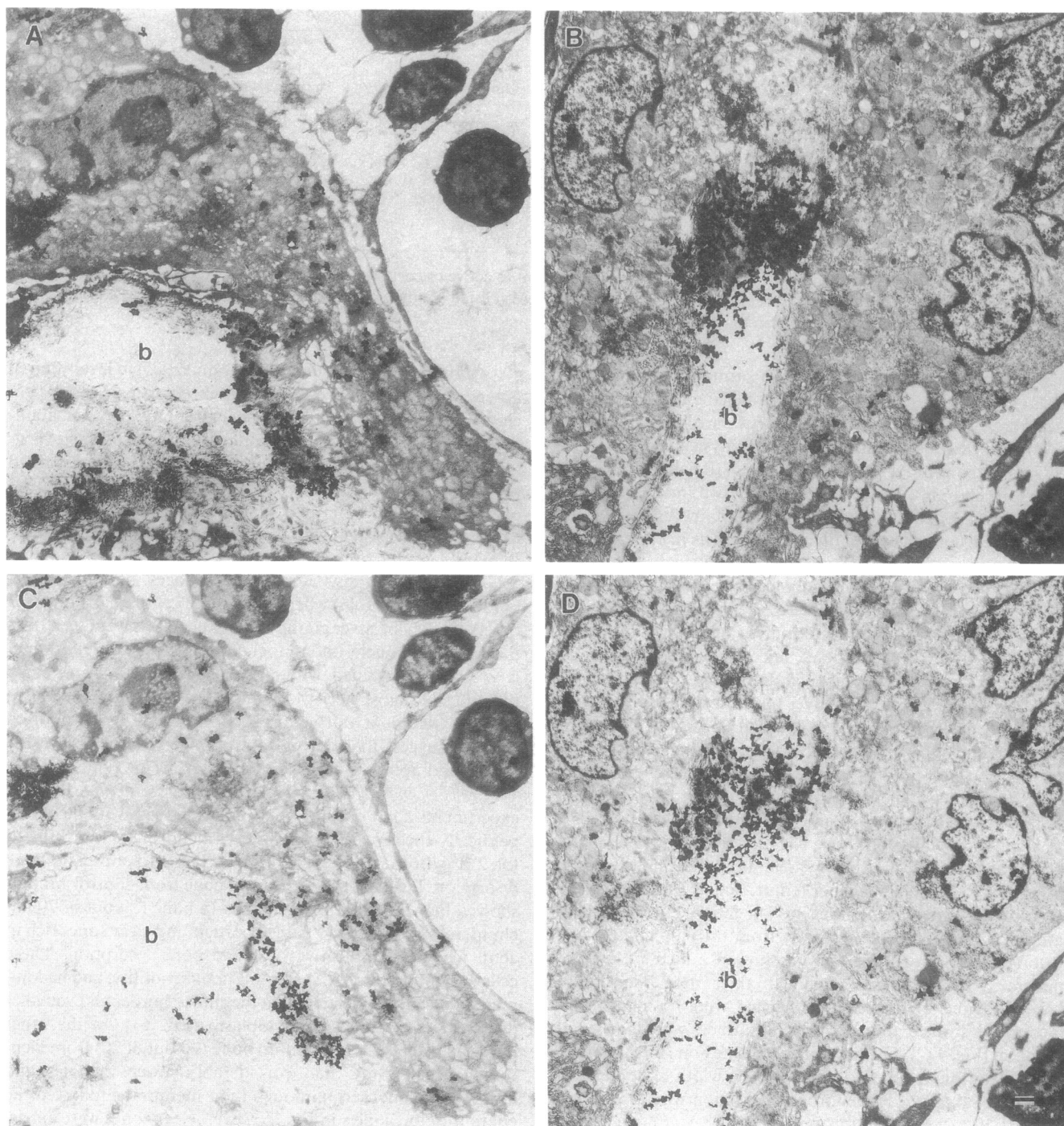


**Figure 5.** Autoradiography of ultrathin sections. Electron microscopy of rats 1 d postinjection confirmed the [ $^3\text{H}$ ]alendronate labelling of resorbing surfaces and osteoclasts. *C* and *D* are lighter exposures of *A* and *B*, respectively, to reveal the silver granules. Heavy labelling of silver granules was associated with bone at the osteoclast interface (*A*, *B*) with some granules over osteoclasts but not other cells (*C*, *D*). The majority (56%) of the granules over osteoclasts were in the proximity of vacuoles but some granules were associated with nuclei and mitochondria or over cytoplasm. These micrographs suggest that osteoclasts are able to dissociate the [ $^3\text{H}$ ]alendronate from the bone surface. Micrometer: 1  $\mu\text{m}$ .

the presence of alendronate on resorption surfaces interferes with ruffled border formation at the bone surface but not attachment to bone.

*Alendronate inhibition of bone resorption by isolated osteoclasts in culture.* To enable the study of alendronate action in culture, its effect on the resorption of [ $^3\text{H}$ ]proline-labeled bone

particles by chicken osteoclasts was compared to its effect on the resorption of bone slices by rat osteoclasts. As seen in Fig. 7, alendronate was equally effective in both cases in inhibiting bone resorption with an  $\text{EC}_{50}$  of  $\sim 0.1 \mu\text{M}$ . Transient incubation of the chicken osteoclasts in the absence of bone with  $0.1 \mu\text{M}$  alendronate for 5 min at  $37^\circ\text{C}$  had no effect on resorption.

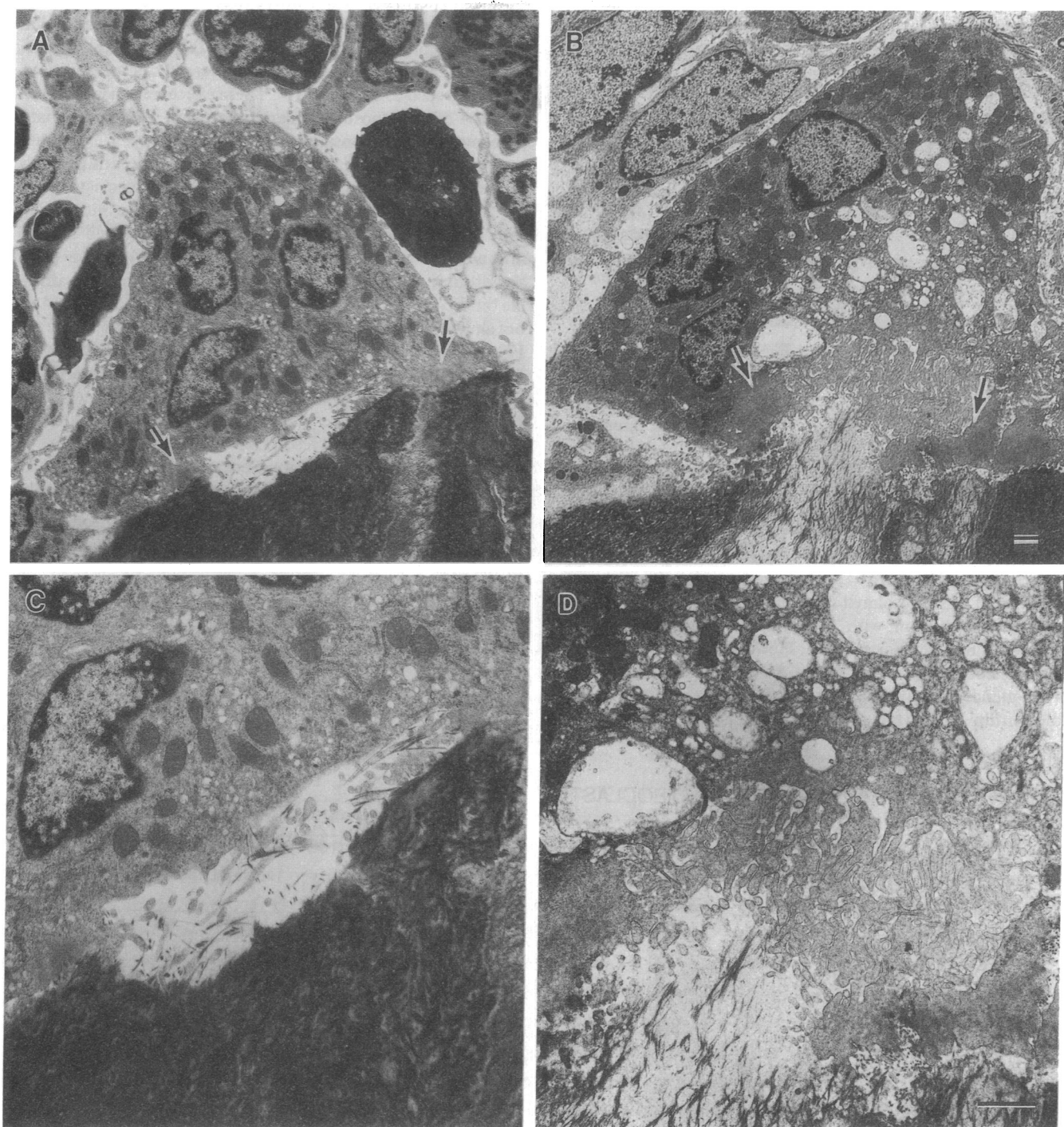


**Figure 6.** Electron microscopy of osteoclasts in PTHrP infused adult rats. Distal tibiae of adult rats infused with PTHrP (1–34) NH<sub>2</sub> given a therapeutic dose of 0.4 mg/kg alendronate (A, C) were examined by electron microscopy. Osteoclasts in these animals were attached to bone with clear zones (arrows, A) but deficient in ruffled border formation (close up, C). By contrast, osteoclasts in control rats were active in resorption as evidenced by the actin rich clear zone (arrows, B), ruffled border (close up, D) and numerous cytoplasmic vacuoles. In alendronate-injected rats 20/20 osteoclasts lacked ruffled borders but were attached to bone with clear zones. Micrometer: 1  $\mu$ m.

*Alendronate effects on osteoclast cyclic AMP and intracellular calcium.* Since a rise in intracellular cyclic AMP was shown to mediate calcitonin inhibition of osteoclastic activity (54), we examined the effects of alendronate on adenylate cyclase activity in isolated chicken osteoclasts. The bisphosphonates alendronate, etidronate, and pamidronate at 0.1 mM and lower

concentrations had no significant effect on cyclic AMP levels, which increased in response to 1  $\mu$ M prostaglandin E<sub>2</sub> (Fig. 8).

A rise in intracellular calcium was proposed to act as an inhibitory signal for osteoclast activity (55–57). We therefore examined the effect of alendronate on cytosolic calcium in isolated chicken and rat osteoclasts, loaded with Fura-2. In the

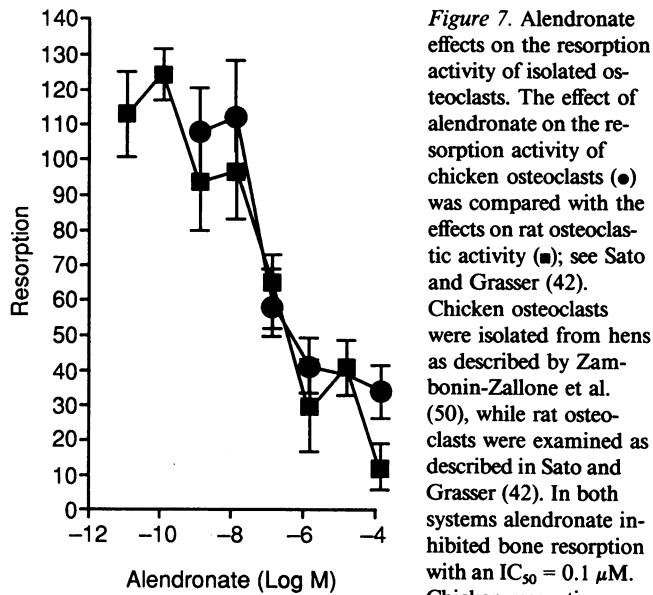


**Figure 7.** Alendronate effects on the resorption activity of isolated osteoclasts. The effect of alendronate on the resorption activity of chicken osteoclasts (●) was compared with the effects on rat osteoclastic activity (■); see Sato and Grasser (42). Chicken osteoclasts were isolated from hens as described by Zamboni-Zallone et al. (50), while rat osteoclasts were examined as described in Sato and Grasser (42). In both systems alendronate inhibited bone resorption with an  $IC_{50} = 0.1 \mu M$ . Chicken resorption

(100%) varied from 19.1 to 23.3  $\mu g$  bone/well for 700–1,500 osteoclasts/cm<sup>2</sup> (mean $\pm$ SEM) ( $n = 7$ ). Rat resorption (100%) varied from 54–252 pits/bone slice, mean $\pm$ SEM ( $n = 7$ ).

majority of freshly isolated (within one day) chicken and rat osteoclasts perfusion with 0.1 mM alendronate caused no changes in intracellular calcium. However, in some cells (17% of rat osteoclasts,  $n = 36$ , and in 29% of chicken osteoclasts,  $n = 55$ ) alendronate increased intracellular calcium two to five-fold within 600 s (Fig. 9 B). By contrast, all osteoclasts re-

#### ADENYLATE CYCLASE ACTIVITY IN OSTEOCLASTS

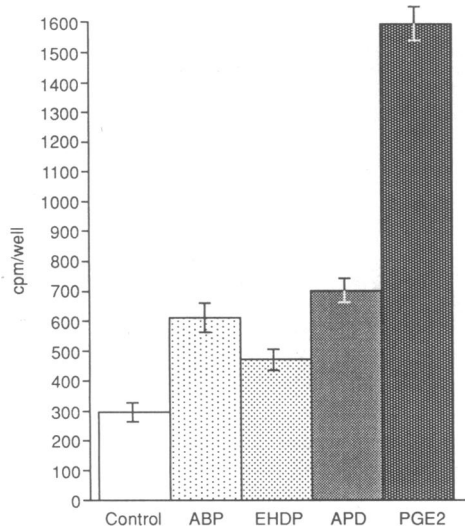


**Figure 8.** Adenylate cyclase activity in chicken osteoclasts. Chicken osteoclasts were incubated with 1  $\mu Ci$  [<sup>3</sup>H]adenine for 2 h at 37°C, washed, and then incubated with 1 mM isobutyl methylxanthine in the absence or presence of 0.1 mM ABP, EHDP, APD, or 1  $\mu M$  prostaglandin E<sub>2</sub> for 10 min. [<sup>3</sup>H] cAMP was column separated from other nucleotides and counted as described previously by Salomon et al. (53). For three sets of experiments ( $n = 3-4$  each), no significant cyclase response was observed for ABP, EHDP, or APD compared to PGE<sub>2</sub> (mean  $\pm$  SD). □, basal; ▤, ABP; ▥, EHDP; ▧, APD; ▨, PGE<sub>2</sub>.

sponded to perfusion with 5 mM extracellular calcium or 4  $\mu M$  BR-A23187 calcium ionophore by an increase in intracellular calcium as previously reported (55–57). Additional experiments indicate that alendronate also increases permeability to other ions such as NH<sub>4</sub> and H<sup>+</sup>. These effects increase with the duration of the exposure to alendronate and with alendronate concentration in a nonsaturable fashion (Zimolo, Z., personal communication). The observed time and concentration dependence may explain the low proportion of osteoclasts showing increases in intracellular calcium at 10-min incubation with 0.1 mM alendronate. No effects were observed at 0.01 mM alendronate (data not shown). Attempts to estimate [<sup>3</sup>H]-alendronate binding to chicken osteoclasts showed no saturable binding, which increased substantially above 0.5 mM (data not shown). This concentration was previously shown to be the EC<sub>50</sub> for rat osteoclast cytotoxicity (42), possibly due to a concentration and time-dependent increase in ion permeability. Taken together these data suggest that neither cAMP nor intracellular calcium act as second messengers for alendronate-mediated inhibition of bone resorption which appears to be due to membrane leakage to small ions, occurring at free alendronate concentrations of 0.1–1 mM. In vivo these effects should be

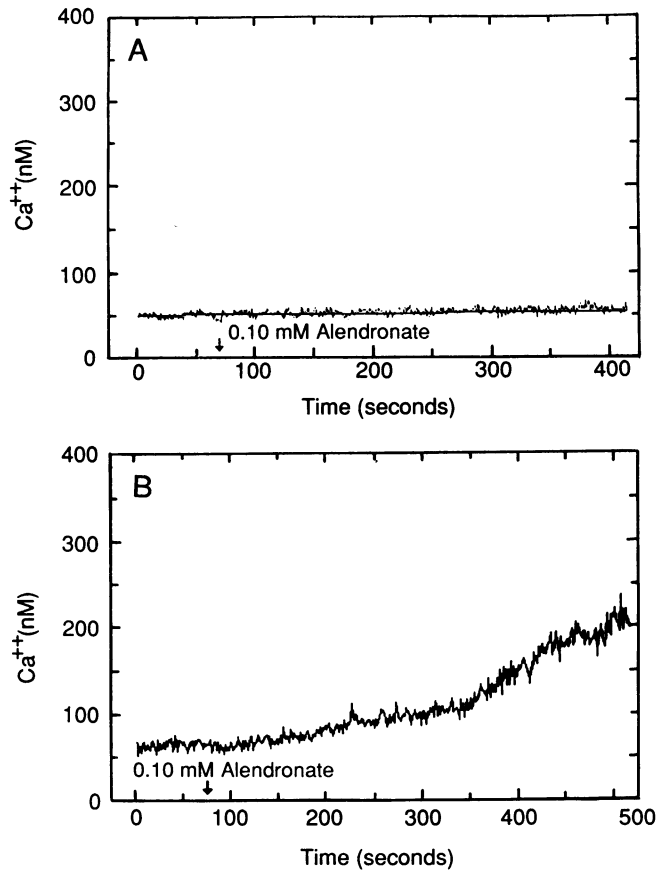


**Figure 9.** Alendronate effects on cytosolic Ca<sup>2+</sup>. The fluorescence emission of osteoclasts loaded with Fura 2 perfused with 0.1 mM alendronate were examined at 348/370 nm excitation. 71% of freshly isolated chicken and 83% of rat osteoclasts showed no response to alendronate perfusion, as seen in A. However, 29% of chicken osteoclasts (within 1 d of isolation) showed a highly variable elevation of Ca<sup>2+</sup> within 6 min of addition, as seen in B–C. Similar data were obtained for 17% of the rat osteoclasts; chicken osteoclasts examined after 6 d in culture showed no response.



limited and self-contained, since once acidification stops the alendronate concentration should drop below those levels.

## Discussion

Bisphosphonates are nonhydrolyzable analogues of pyrophosphate, which reduce the dissolution rate of the bone mineral hydroxyapatite (31). Some bisphosphonates also reduce bone resorption (31); however, this effect cannot be attributed to the reduction in mineral solubility since the potency of various bisphosphonates in the two assays varies considerably (58). It is recognized that bisphosphonates act on the bone cells, but their mode of action is still poorly understood.

All bisphosphonates bind to hydroxyapatite by virtue of the PCP structure, which accounts for their rapid uptake in bone and their selective action on the skeleton. The PCP structure probably also accounts for the metabolic stability of these compounds and their relatively rapid clearance in the urine. Skeletal uptake of alendronate in rats reaches 90% of peak values within 1 h of intravenous or oral administration (58a).

The binding of alendronate to bone particles *in vitro* was saturable and reversible. The apparent dissociation constant of  $\sim 1$  mM at pH 7 is consistent with the binding of the phosphate groups to calcium on the surface of the apatite crystals, and a capacity of  $\sim 100$  nmol/mg bone (dry weight), is consistent with the large surface of accessible hydroxyapatite crystals in bone powder.

If the *in vitro* observations are extrapolated to the whole human skeleton, its capacity for alendronate at saturation would be 90 g. This figure contrasts with a skeletal uptake of 2.5–10 mg, which effectively controls hypercalcemia of malignancy (46) and reduces alkaline phosphatase in Paget's disease (12). The explanation for this discrepancy lies most likely in the localization of the compound.

*In vitro* etidronate competes for alendronate binding with similar affinity, indicating that the 100–500-fold difference in the bone resorption inhibitory activity of the two bisphosphonates is not due to a difference in bone binding but possible due to a difference in their mode of action or distribution *in vivo*. The strong pH dependence of alendronate binding to bone particles, resulting in 50% release at pH 3.5, is expected from the interaction of phosphate with hydroxyapatite. Consequently, if the osteoclasts form a clear zone on alendronate-containing bone surfaces, as shown in Fig. 6, and acidify the osteoclast bone interface (59–61), the local concentration of alendronate released in the resorption space would be substantially higher than that present in the circulation following alendronate administration and could reach 0.1–1 mM (see below).

24 h after the administration of a single dose of [ $^3$ H]-alendronate ( $\sim 0.4$  mg/kg) over 70% of the osteoclast surface was densely labelled. By comparison only 2% of the bone forming surface and  $\sim 13\%$  of all other surfaces, which contain eroded surfaces without osteoclasts and resting surfaces, were similarly labelled. This preferential localization of alendronate could be due to the exposure of hydroxyapatite at sites prepared for or undergoing bone resorption and the accessibility of these bone surfaces to substances in the circulation. About 28% of the osteoclastic surface remained unlabelled, possibly representing sites in which the exposure of hydroxyapatite and initiation of resorption occurred after [ $^3$ H]-alendronate uptake in bone, which takes  $< 2$  h. About half the bone formation surface label at levels higher than the diffuse label on the

bone surface but lower than the intense label seen under the osteoclasts.

The lower level of [ $^3$ H]-alendronate uptake on bone formation surfaces could be due to the lower accessibility of the hydroxyapatite behind the osteoid to alendronate, which is a larger and more polar molecule than technetium methyl diphosphonate, which is used for bone scanning and localizes extensively on bone formation surfaces. The resting, eroded, and all other surfaces were pooled and accounted for about half the total bone surface. About 13% of that surface was densely labelled and  $\sim 11\%$  was moderately labelled. The dense label was more frequently observed on surfaces sparsely covered by cells and could represent sites about to be resorbed. Collagenase digestion, which may precede resorption (62), could expose hydroxyapatite and lead to higher uptake of label. Overall, 10% of the bone surface was densely and 27% moderately labelled. Assuming that the amount of alendronate in the former was about fivefold higher than in the latter,  $\sim 65\%$  of the alendronate was found on densely labelled surfaces and a third of that under osteoclasts apposed to bone.

Based on the radioactivity in the histological sections, after ascertaining that no radioactivity was released during fixation, processing, and staining, and the section width of  $0.4$   $\mu\text{m}$ , the osteoclast surface contained  $\sim 1.6 \times 10^{-3}$  fmol/ $\mu\text{m}^2$ . If 50% would be released during the acidification produced by osteoclasts, as suggested by the *in vitro* experiments, into a space of  $1$   $\mu\text{m}$  deep, the local concentration under the ruffled border would be 0.8 mM. However, as soon as acidification stops the bisphosphonate should reabsorb to the hydroxyapatite and the free concentration should drop substantially.

6 d after [ $^3$ H]-alendronate injection the bones contained virtually the same amount of radioactivity as at 24 h, consistent with the long half-life of bisphosphonates in bone. The label was, however, at a considerable distance from the epiphyseal plate (600–1,000  $\mu\text{m}$ ), indicating unimpaired longitudinal growth and was buried inside the bone, indicating bone formation on top of alendronate containing surfaces.

Electron micrographs of the osteoclast bone interface from [ $^3$ H]-alendronate-treated animals confirmed the presence of dense label on the osteoclastic surface and suggested that local acidification could occur since an apparently normal clear zone was seen in close apposition to bone. Ruffled border could be recognized at this interface; however, it was less sharply defined than other plasma membranes in the same section. Moreover, silver grains could be detected over these osteoclasts, but no other cells in these sections, suggesting penetration of alendronate into the cells and disruption of membrane integrity.

In animals infused with PTHrP the number of osteoclasts increased  $\sim 10$ -fold (63) and alendronate (two subcutaneous injections of 0.4 mg/kg) did not interfere with osteoclast recruitment. On electron microscopic examination 20 out of 20 osteoclasts in the animals lacked ruffled border at the osteoclast bone interface as observed by Plasmans et al. (41) after pamidronate treatment, while clear zone could be seen in several of these cells. 20 osteoclasts surveyed in the control bones had identifiable ruffled borders. Taken together these findings support the hypothesis that after administration alendronate binds to exposed hydroxyapatite surfaces, osteoclasts attach to these surfaces via integrins (64) and may start resorbing, acidification causes alendronate release within the space defined by the clear zone, the rise in alendronate concentration interferes with ruffled border membrane function, stopping resorption. This

seems to be a self-contained process, which does not kill the osteoclasts, since the number of osteoclasts in alendronate-treated animals under conditions which increase bone resorption, such as estrogen deficiency (45), or secondary hyperparathyroidism (data not shown), as well as in this study, was not reduced and disintegrating osteoclasts were never observed.

These observations were confirmed by experiments in culture. Alendronate did not inhibit osteoclast attachment to bone particles (data not shown), consistent with the presence of clear zone in alendronate-treated animals. However, alendronate inhibited bone resorption by both rat and chick osteoclasts in culture with very similar dose-response curves ( $EC_{50}$  around  $0.1 \mu\text{M}$ ). We also estimated the amount of alendronate at the osteoclast bone interface in this system. Bone slices with a total macroscopic surface area of  $\sim 42 \text{ mm}^2$  bound  $0.05 \text{ nmol}$  of alendronate when incubated with a  $0.1\text{-}\mu\text{M}$  solution. Assuming random distribution the bone slice surface contained  $\sim 1.25 \times 10^{-3} \text{ fmol}/\mu\text{m}^2$ . If 50% of this material was released locally into a sealed space of  $500\text{--}1,000 \mu\text{m}^3$ , the alendronate concentration would be  $0.3\text{--}0.6 \text{ mM}$ . These figures are in good agreement with the amounts of alendronate on osteoclastic surfaces, estimated from the tissue distribution of [ $^3\text{H}$ ]alendronate, after the in vivo administration of an effective antiresorptive dose of alendronate ( $0.4 \text{ mg/kg}$ ), as described in Methods.

At  $0.1 \text{ mM}$  alendronate we found that between 20 and 30% of rat and chicken osteoclasts showed increased leakiness to calcium within 10 min exposure. Alendronate also caused increased leakiness to  $\text{NH}_4$  and  $\text{H}^+$ , which was both dose dependent between  $0.1$  and  $1 \text{ mM}$  and increased with time between 10 and 30 min (Zimolo, Z., personal communication). Furthermore, alendronate binding to chicken osteoclasts was nonsaturable and increased above  $0.5 \text{ mM}$  (data not shown), the  $EC_{50}$  for osteoclast 24-h cytotoxicity (42). Taken together these findings suggest that exposure of osteoclast membranes to alendronate above  $0.1 \text{ mM}$  increases the permeability to calcium and probably other ions. Time and dose dependence of this effect may explain why only 20–30% of the rat and chicken osteoclasts showed increases in intracellular calcium in the experiments reported here. If aminobisphosphonates increase calcium leakage they may stop osteoclast activity before producing irreversible damage to these cells. Once osteoclastic activity is inhibited, acidification stops, the bisphosphonate concentration is reduced, membrane integrity seems to be restored, as suggested by the electron microscopic observations described above. This would not lead to osteoclast death; indeed, unlike the reports for treatment with dichloromethyl bisphosphonate (33) and hydroxy ethylidene bisphosphonic acid (65), the number of osteoclasts was not reduced after aminobisphosphonate treatment. This could explain the different effects of aminohydroxypropylidene bisphosphonate (APD) and dichloromethylene bisphosphonate on rat macrophage bone resorption in culture (66).

The findings described above are consistent with numerous effects of bisphosphonates on cells in culture, which could be caused by interference with the integrity of the cell membrane (67), such as increased prostaglandin synthesis (68) or inhibition of macrophage migration (69). The findings of Carano et al., showing that exposure to  $11 \mu\text{M}$  bisphosphonate for 72 h inhibits cell metabolism (34) and of Felix et al. (70) showing cellular uptake of bisphosphonates are also consistent with our findings.

In conclusion, the working hypothesis for the mechanism of action of alendronate supported by the findings presented

above is: (a) preferential uptake of alendronate on exposed hydroxyapatite surfaces prepared for bone resorption; (b) acidification produced during the initiation of resorption causes the local release of alendronate, which may reach a concentration of  $0.1\text{--}1 \text{ mM}$  within the space confined by the clear zone; (c) at this concentration alendronate may increase the "leakiness" of the ruffled border to ions; (d) resorption stops and the cells lose ruffled border.

## References

1. Fleisch, H. 1987. Bisphosphonates—history and experimental basis. *Bone (NY)*. 8(Suppl.):523–528.
2. Smith, R., R. G. G. Russell, and M. Bishop. 1971. Diphosphonates and Paget's disease of bone. *Lancet*. i:945–947.
3. Meunier, P. J., C. Alexandre, C. Edouard, L. Mathieu, M. C. Chapuy, C. Bressot, E. Vignon, and U. Trechsel. 1979. Effects of disodium dichloromethylene diphosphonate on Paget's disease of bone. *Lancet*. i:489–492.
4. Frijlink, W. B., O. L. M. Bijvoet, J. te Veide, and G. Heynen. 1979. Treatment of Paget's disease with (3-amino-1-hydroxypropylidene)-1,1-bisphosphonate (APD). *Lancet*. i:799–803.
5. Russell, R. G. G., R. Smith, C. J. Preston, R. S. Walton, and C. G. Woods. 1974. Diphosphonates in Paget's disease. *Lancet*. i:894–898.
6. Canfield, R., W. Rosner, J. Skinner, J. McWhorter, L. Resnick, F. Feldman, S. Kammermans, J. Ryan, M. Kunigonis, and W. Bohne. 1977. Diphosphonate therapy of Paget's disease of bone. *J. Clin. Endocrinol. & Metab.* 44:96–106.
7. Douglas, D. L., T. Tuckworth, R. G. G. Russell, J. A. Kanis, C. J. Preston, F. E. Preston, M. A. Prenton, and J. S. Woodhead. 1980. Effect of dichloromethylene diphosphonate on Paget's disease of bone and hypercalcaemia due to primary hyperparathyroidism or malignant disease. *Lancet*. i:1043–1047.
8. Harinck, H. I. J., S. E. Papapoulos, H. J. Blanksma, A. J. Moolenaar, L. Vermeij, and O. L. M. Bijvoet. 1987. Paget's disease of bone: early and late responses to three different modes of treatment with aminohydroxypropylidene bisphosphonate (APD). *Brit. Med. J.* 295:1301–1305.
9. Pedrazzoni, M., E. Palummeri, G. Ciotti, L. Davoli, G. Pioli, G. Girasole, and M. Passeri. 1989. Short-term effects on bone and mineral metabolism of 4-amino-1-hydroxybutylidene-1,1-diphosphonate (ABDP) in Paget's disease of bone. *Bone Miner.* 7:301–307.
10. Stone, M. D., A. B. Hawthorne, D. Kerr, G. Webster, and D. J. Hosking. 1990. Treatment of Paget's disease with intermittent low-dose infusions of disodium pamidronate (APD). *J. Bone Miner. Res.* 5:1231–1235.
11. O'Doherty, D. P., D. R. Bickerstaff, E. V. McCloskey, N. A. T. Hamdy, M. N. C. Beneton, S. Harris, M. Mian, and J. A. Kanis. 1990. Treatment of Paget's disease of bone with amino-hydroxybutylidene bisphosphonate. *J. Bone Miner. Res.* 5:483–491.
12. Adami, S. 1986. Treatment of Paget's disease of bone with intravenous 4-amino-1-hydroxybutylidene-1,1-bisphosphonate. *Calcif. Tissue Int.* 39:226–233.
13. van Holten-Verzantvoort, A., O. L. M. Bijvoet, F. J. Cleton, J. Termans, H. M. Kroon, H. I. J. Harinck, P. Vermey, J. W. F. Elte, J. P. Neijt, L. V. A. M. Beex, and G. G. Blijham. 1987. Reduced morbidity from skeletal metastases in breast cancer patients during long-term bisphosphonate (APD) treatment. *Lancet*. ii:983–985.
14. Morton, A. R., J. A. Cantrill, G. V. Pillai, A. McMahon, D. C. Anderson, and A. Howell. 1988. Sclerosis of lytic bone metastases after disodium aminohydroxypropylidene bisphosphonate (APD) in patients with breast carcinoma. *Br. Med. J.* 297:772–773.
15. Elomaa, I., C. Blomquist, L. Porkka, T. Holmstrom, T. Taube, C. Lamberg-Allardt, and G. H. Borgstrom. 1988. Clodronate for osteolytic metastases due to breast cancer. *Biomed. & Pharmacother.* 42:111–116.
16. Merlini, G., G. A. Parrinello, L. Piccinini, F. Crema, M. L. Fiorentini, A. Riccardi, F. Pavesi, F. Novazzi, V. Silingardi, and E. Ascari. 1990. Long-term effects of parenteral dichloromethylene bisphosphonate (CL2MBP) on bone disease of myeloma patients treated with chemotherapy. *Hematol. Oncol.* 3:23–30.
17. Attardo-Parrinello, G., G. Merlini, F. Pavesi, M. L. Fiorentini, and E. Ascari. 1987. Effects of a new aminodiphosphonate in patients with osteolytic lesions from metastases and myelomatosis. *Arch. Intern. Med.* 147:1629–1633.
18. Siris, E. S., W. H. Sherman, D. C. Baquiran, J. P. Schatterer, E. F. Osserman, and R. E. Canfield. 1980. Effects of dichloromethylene diphosphonate on skeletal mobilization of calcium in multiple myeloma. *N. Engl. J. Med.* 302:310–315.
19. Jung, A. 1982. Comparison of two parenteral diphosphonates in hypercalcaemia of malignancy. *Am. J. Med.* 72:221–226.
20. Sleeboom, H. P., O. L. M. Bijvoet, A. J. van Oosterom, J. H. Gled, and J. H. L. O'Riordan. 1983. Comparison of intravenous (3-amino-1-hydroxypropylidene)-1,1-bisphosphonate and volume repletion in tumour-induced hypercalcaemia. *Lancet*. i:239–243.

21. Percival, R. C., A. D. Paterson, A. J. P. Yates, B. J. Beard, D. L. Douglas, F. E. Neal, R. G. G. Russell, and J. A. Kanis. 1985. Treatment of malignant hypercalcaemia with clodronate. *Br. J. Cancer* 51:665-669.
22. Ralston, S. J., M. D. Gardner, F. J. Dryborough, A. S. Jenkins, R. A. Cowan, and I. T. Boyle. 1985. Comparison of aminohydroxy-propylidene diphosphonate, mitramycin and corticosteroids/calcitonin in treatment of cancer-associated hypercalcaemia. *Lancet*. ii:907-910.
23. Ralston, S. H., U. Patel, W. D. Fraser, S. J. Gallacher, F. J. Dryburgh, R. A. Cowan, and I. T. Boyle. 1989. Comparison of three intravenous bisphosphonates in cancer-associated hypercalcaemia. *Lancet*. ii:1180-1182.
24. Davis, J. R. E., and D. A. Heath. 1989. Comparison of different dose regimes of aminohydroxypropylidene-1,1-bisphosphonate (APD) in hypercalcaemia of malignancy. *Br. J. Clin. Pharmacol.* 28:269-274.
25. Valkema, R., F.-J. F. E. Vismans, S. E. Papapoulos, E. K. J. Pauwels, and O. L. M. Bijvoet. 1989. Maintained improvement in calcium balance and bone mineral content in patients with osteoporosis treated with the bisphosphonate APD. *Bone Miner.* 5:183-192.
26. Reid, I. R., C. J. Alexander, A. R. King, and H. K. Ibertson. 1988. Prevention of steroid-induced osteoporosis with (3-amino-1-hydroxypropylidene)-1,1-bisphosphonate (APD). *Lancet*. i:143-146.
27. Reid, I. R., B. A. Schooler, and A. W. Stewart. 1990. Prevention of glucocorticoid-induced osteoporosis. *J. Bone Miner. Res.* 5:619-623.
28. Reginster, J. Y., R. Deroisy, D. Denis, J. Collette, M. P. Lecart, N. Sarlet, D. Ethgen, and P. Franchimont. 1989. Prevention of postmenopausal bone loss by tiludronate. *Lancet*. ii:1469-1471.
29. Storm, T., G. Thamsborg, T. Steiniche, H. K. Genant, and O. H. Sorensen. 1990. Effect of intermittent cyclical etidronate therapy on bone mass and fracture rate in women with postmenopausal osteoporosis. *N. Engl. J. Med.* 322:1265-1271.
30. Watts, N. B., S. T. Harris, H. K. Genant, R. D. Wasnich, P. D. Miller, R. D. Jackson, A. A. Licata, P. Ross, G. C. Woodson, M. J. Yanover, et al. 1990. Intermittent cyclical etidronate treatment of postmenopausal osteoporosis. *N. Engl. J. Med.* 323:73-79.
31. Fleisch, J., R. G. G. Russell, and M. D. Francis. 1969. Diphosphonates inhibit hydroxyapatite dissolution in vitro and bone resorption in tissue culture and in vivo. *Science (Wash. DC)*. 165:1262-1264.
32. Boonekamp, P. M., L. J. A. van der Wee-Pals, M. M. L. van Wijk-van Lennep, C. W. Thesingh, and O. L. M. Bijvoet. 1986. Two modes of action of bisphosphonates on osteoclastic resorption of mineralized matrix. *Bone Miner.* 1:27-39.
33. Flanagan, A. M., and T. J. Chambers. 1989. Dichloromethylenebisphosphonate (Cl2MBP) inhibits bone resorption through injury to osteoclasts that resorb Cl2MBP-coated bone. *Bone Miner.* 6:33-43.
34. Carano, A., S. L. Teitelbaum, J. D. Konsek, P. H. Schlesinger, and H. C. Blair. 1990. Bisphosphonates directly inhibit the bone resorption activity of isolated avian osteoclasts in vitro. *J. Clin. Invest.* 85:456-461.
35. Lowik, C. W. G. M., G. van der Pluijm, L. J. A. van der Wee-Pals, H. Bloys-van Treslong-de Groot, and O. L. M. Bijvoet. 1988. Migration and phenotypic transformation of osteoclast precursors into mature osteoclasts. *J. Bone Miner. Res.* 3:185-192.
36. Cecchini, M. G., R. Felix, H. Fleisch, and P. H. Cooper. 1987. Effect of bisphosphonates on proliferation and viability of mouse bone marrow-derived macrophages. *J. Bone Miner. Res.* 2:135-142.
37. Hughes, D. E., B. R. MacDonald, R. G. G. Russell, and M. Gowen. 1989. Inhibition of osteoclast-like cell formation by bisphosphonates in long-term cultures of human bone marrow. *J. Clin. Invest.* 83:1930-1935.
38. Papapoulos, S. E., K. Hoekman, C. W. G. M. Lowik, P. Vermeij, and O. L. M. Bijvoet. 1989. Application of an *in vitro* model and a clinical protocol in the assessment of the potency of a new bisphosphonate. *J. Bone Miner. Res.* 4:775-781.
39. Cecchini, M. G., and H. Fleisch. 1990. Bisphosphonates in vitro specifically inhibit, among the hematopoietic series, the development of the mouse mononuclear phagocyte lineage. *J. Bone Miner. Res.* 5:1019-1027.
40. Miller, S. C., and W. S. S. Jee. 1979. The effect of dichloromethylene diphosphonate, a pyrophosphate analog, on bone and bone cell structure in the growing rat. *Anat. Rec.* 193:439-462.
41. Plasmans, C. M. T., P. H. K. Jap, W. Kuypers, and T. J. J. Slooff. 1980. Influence of a diphosphonate on the cellular aspect of young bone tissue. *Calcif. Tissue Int.* 32:247-256.
42. Sato, M., and W. Grasser. 1990. Effects of bisphosphonates on isolated rat osteoclasts as examined by reflected light microscopy. *J. Bone Miner. Res.* 5:31-40.
43. Schenk, R., P. Egli, H. Fleisch, and S. Rosini. 1986. Quantitative morphometric evaluation of the inhibitory activity of new aminobisphosphonates on bone resorption in the rat. *Calcif. Tissue Int.* 38:342-349.
44. Thompson, D. D., J. G. Sedor, M. Weinreb, S. Rosini, and G. A. Rodan. 1990. Aminohydroxybutane bisphosphonate inhibits bone loss due to immobilization in rats. *J. Bone Miner. Res.* 5:279-286.
45. Sedor, J. G., H. A. Quartuccio, and D. D. Thompson. 1991. The bisphosphonate alendronate (MK-217) inhibits bone loss due to ovariectomy in rats. *J. Bone Miner. Res.* 6:339-346.
46. Burssens, A., G. J. Gertz, R. M. Francis, J. R. Tucci, and F. R. Singer. 1990. A double-blind, placebo controlled, rising multiple dose trial of oral alendronate in Paget's Disease. *J. Bone Miner. Res.* 5(Suppl. 2):S239.
47. Rouleau, M. F. 1986. Parathyroid hormone binding in vivo to renal, hepatic and skeletal tissues of the rat using a radioautographic approach. *Endocrinology*. 118:919-931.
48. Kopriwa, B. M. 1975. A comparison of various procedures for fine grain development in electron microscopic radioautography. *Histochemistry*. 44:201-224.
49. Venable, J. A., and R. Coggeshall. 1965. A simplified lead citrate stain for use in electron microscopy. *J. Cell Biol.* 25:407.
50. Zamboni-Zallone, A., A. Teti, and M. V. Primavera. 1982. Isolated osteoclasts in primary culture: first observations on structure and survival in culture media. *Anat. Embryol.* 165:405-413.
51. Blair, H. C., A. J. Kahn, E. C. Crouch, J. J. Jeffrey, and S. L. Teitelbaum. 1986. Osteoclasts resorb the organic and inorganic components of bone. *J. Cell Biol.* 102:1164-1172.
52. Arnett, T. R., and D. W. Dempster. 1987. A comparative study of disaggregated chick and rat osteoclasts in vitro: effects of calcitonin and prostaglandins. *Endocrinology*. 120:602-608.
53. Salomon, Y., C. Londos, and M. Rodball. 1974. A highly sensitive adenylate cyclase assay. *Anal. Biochem.* 58:541-548.
54. Nicholson, C. G., J. M. Moseley, P. M. Sexton, F. A. O. Mendelsohn, and T. J. Martin. 1986. Abundant calcitonin receptors in isolated rat osteoclasts. Biochemical and autoradiographic characterization. *J. Clin. Invest.* 78:335-360.
55. Miyachi, A., K. A. Hruska, E. M. Greenfield, R. Duncan, J. Alvarez, R. Barattolo, S. Colucci, A. Zamboni-Zallone, S. L. Teitelbaum, and A. Teti. 1990. *J. Cell Biol.* 111:2543-2552.
56. Malgaroli, A., J. Meldolesi, A. Zamboni-Zallone, and A. Teti. 1989. Control of cytosolic free calcium in rat and chicken osteoclasts. *J. Biol. Chem.* 264:14342-14347.
57. Zaida, M., H. K. Datta, A. Patchell, B. Moonga, and I. MacIntyre. 1989. Calcium-activated intracellular calcium elevation: a novel mechanism of osteoclast regulation. *Biochem. Biophys. Res. Commun.* 159:68-71.
58. Seitsma, W. K., F. H. Ebetino, A. M. Savagno, and J. A. Bevan. 1989. Antiresorptive dose-response relationships across three generations of bisphosphonates. *Drugs Exp. Clin. Res.* 15:389-396.
- 58a. Lin, J. H., D. E. Duggan, I.-W. Chen, and R. L. Ellsworth. 1991. Physiological disposition of alendronate, a potent antiosteolytic bisphosphonate, in laboratory animals. *Drug Metab. Dispos.* 19:926-932.
59. Baron, R., L. Neff, D. Louvard, and P. J. Courtoy. 1985. Cell-mediated extracellular acidification and bone resorption: evidence for a low pH in resorbing lacunae and localization of a 100-kD lysosomal membrane protein of the osteoclast ruffled border. *J. Cell Biol.* 101:2210-2222.
60. Blair, H. C., S. L. Teitelbaum, R. Ghiselli, and S. Gluck. 1989. Osteoclastic bone resorption by a polarized vacuolar proton pump. *Science (Wash. DC)*. 245:855-857.
61. Vaananen, H. K., E.-K. Karhukorpi, K. Sundquist, B. Wallmark, I. Roininen, T. Hentunen, J. Tuukkanen, and P. Lakkakorpi. 1990. Evidence for the presence of a proton pump of the vacuolar H<sup>+</sup>-ATPase type in the ruffled borders of osteoclasts. *J. Cell Biol.* 111:1305-1311.
62. Chambers, T. J., J. A. Darby, and K. Fuller. 1985. Mammalian collagenase predisposes bone surfaces to osteoclastic resorption. *Cell Tissue Res.* 241:671-675.
63. Thompson, D. D., J. G. Sedor, J. E. Fisher, M. Rosenblatt, and G. A. Rodan. 1988. Direct action of the parathyroid hormone-like human hypercalcaemic factor on bone. *Proc. Natl. Acad. Sci. USA*. 85:5673-5677.
64. Sato, M., M. K. Sardana, W. A. Grasser, V. M. Garsky, J. M. Murray, and R. J. Gould. 1990. Echinatin is a potent inhibitor of bone resorption in culture. *J. Cell Biol.* 111:1713-1723.
65. Chappard, D., C. Alexandre, S. Palle, L. Vico, B. V. Morukov, S. S. Rodinova, P. Minaire, and G. Riffat. 1989. Effects of a bisphosphonate (1-hydroxy ethylidene-1,1 bisphosphonic acid) on osteoclast number during prolonged bed rest in healthy humans. *Metabolism (Clin. & Exp.)*. 38:822-825.
66. Reitsma, P. H., S. L. Teitelbaum, O. L. M. Bijvoet, and A. J. Kahn. 1982. Differential action of the bisphosphonates (3-amino-1-hydroxypropylidene)-1,1-bisphosphonate (APD) and disodium dichloromethylene bisphosphonate (Cl2MDP) on rat macrophage-mediated bone resorption in vitro. *J. Clin. Invest.* 70:927-933.
67. Fast, D. K., R. Felix, C. Dowse, W. F. Neuman, and H. Fleisch. 1978. The effects of diphosphonates on the growth and glycolysis of connective tissue cells in culture. *Biochem. J.* 172:97-107.
68. Felix, R., J. D. Bettex, and H. Fleisch. 1981. Effects of diphosphonates on the synthesis of prostaglandins in cultured calvaria cells. *Calcif. Tissue Int.* 33:549-552.
69. Stevenson, P. H., and J. R. Stevenson. 1986. Cytotoxic and migration inhibitory effects of bisphosphonates on macrophages. *Calcif. Tissue Int.* 38:227-233.
70. Felix, R., H. L. Guenther, and H. Fleisch. 1984. The subcellular distribution of [<sup>14</sup>C]dichloromethylenebisphosphonate and [<sup>14</sup>C]1-hydroxyethylidene-1,1-bisphosphonate in cultured calvaria cells. *Calcif. Tissue Int.* 36:108-113.